

Structural basis of intersubunit recognition in elongin BC–cullin 5–SOCS box ubiquitin–protein ligase complexes

Young Kwan Kim,^a Mi-Jeong Kwak,^a Bonsu Ku,^b Hye-Young Suh,^{a,‡} Keehyoung Joo,^c Jooyoung Lee,^c Jae U. Jung^d and Byung-Ha Oh^{a*}

^aDepartment of Biological Sciences, KAIST Institute for the Biocentury, Korea Advanced Institute of Science and Technology, Daejeon 305-701, Republic of Korea, ^bMedical Proteomics Research Center, Korea Research Institute of Bioscience and Biotechnology, Daejeon 305-806, Republic of Korea, ^cSchool of Computational Sciences and Center for In Silico Protein Science, Korea Institute for Advanced Study, Seoul 130-722, Republic of Korea, and ^dDepartment of Molecular Microbiology and Immunology, Keck School of Medicine, University of Southern California, Los Angeles, CA 90089, USA

‡ Current address: Samsung Advanced Institute of Technology, Yongin, Gyeonggi 446-712, Republic of Korea.

Correspondence e-mail: bhoh@kaist.ac.kr

The cullin–RING ubiquitin ligases are multisubunit complexes that ubiquitinate various proteins. Six different cullins encoded by the human genome selectively pair with different adaptors and substrate receptors. It is presently poorly understood how cullin-2 (Cul2) and cullin-5 (Cul5) associate specifically with their adaptor elongin BC and a SOCS-box-containing substrate receptor. Here, crystallographic and mutational analyses of a quaternary complex between the N-terminal half of Cul5, elongin BC and SOCS2 are reported. Cul5 interacts extensively with elongin BC *via* residues that are highly conserved in Cul2 but not in other cullins. Cul5 also interacts with SOCS2, but *via* only two residues, Pro184 and Arg186, which are located in the C-terminal part of the SOCS box called the Cul5 box. Pro184 makes a ring-to-ring interaction with Trp53 of Cul5, which is substituted by alanine in Cul2. This interaction is shown to contribute significantly to the overall binding affinity between Cul5 and SOCS2–elongin BC. This study provides structural bases underlying the specificity of Cul5 and Cul2 for elongin BC and their preferential association with Cul5 or Cul2 box-containing substrate receptors.

Received 12 March 2013

Accepted 24 April 2013

PDB Reference: SOCS2–
elongin BC–Cul5N(RD), 4jgh

1. Introduction

A wide variety of eukaryotic proteins are post-translationally modified by conjugation of a single or multiple molecule(s) of ubiquitin, a small protein composed of about 76 amino acids. The consequences of ubiquitination vary widely and include degradation, change in activity and change in cellular location of the modified proteins (Hershko & Ciechanover, 1992). The three enzymes E1, E2 and E3 catalyze cascade-like transfers of ubiquitin to a substrate protein. E3 is the ubiquitin ligase, which catalyzes the formation of an isopeptide bond between the C-terminal carboxylate of ubiquitin and a lysine residue of a protein (Pickart, 2001). The cullin–RING ubiquitin ligases comprise a superfamily of multi-subunit RING-class E3 enzymes that commonly contain an elongated arch-shaped cullin scaffold and a RING-domain subunit, Rbx1 or Rbx2 (Kamura *et al.*, 1999; Ohta *et al.*, 1999; Tan *et al.*, 1999). Six different human cullins have been identified: cullin-1 (Cul1), Cul2, Cul3, Cul4A, Cul4B and Cul5 (Bosu & Kipreos, 2008; Villeneuve *et al.*, 2010). In addition, an atypical cullin protein Cul7 has been identified which binds to the F-box-containing protein Fbxw8 (Dias *et al.*, 2002; Ponyeam & Hagen, 2012). They are sequentially folded to form an elongated scaffold with two ends that are separated from each other by about 100 Å. The C-terminal end of the scaffold is the site for

binding Rbx1 or Rbx2, which interacts with the E2 enzyme (Zheng *et al.*, 2002). The other end of the scaffold consists of the N-terminal residues and is the site for binding the adaptor subunit. The adaptor interacts with the substrate receptor that recognizes and binds to a substrate protein. Through these interactions, a substrate protein is brought to a cullin scaffold, on which the transfer of ubiquitin from E2 to the substrate is catalyzed. Cul3 is exceptional in that it binds to the substrate receptor directly (Zimmerman *et al.*, 2010). Recently, using molecular-dynamics simulations, it has been suggested that the cullin scaffolds are flexible and that this flexibility is likely to provide an allosteric regulatory mechanism to facilitate the polyubiquitination of substrates (Liu & Nussinov, 2011).

Elongin B and elongin C form a tightly associated complex and this heterodimer, referred to as elongin BC, serves as the common adaptor subunit for both Cul2 and Cul5 (Duan *et al.*, 1995). Elongin C shares sequence and structural similarity with S-phase kinase-associated protein 1 (Skp1), which is the adaptor protein interacting with Cul1 (Bai *et al.*, 1996). The interaction between Skp1 and Cul1 has been structurally characterized (Zheng *et al.*, 2002). Whereas structural information on how elongin BC binds to Cul2 or Cul5 is unavailable, the elongin C subunit has been presumed to bind Cul2 and Cul5 similarly to the binding of Skp1 by Cul1 (Zheng *et al.*, 2002). Elongin BC recognizes cognate substrate receptors that are characterized by having a conserved C-terminal sequence known as the SOCS box (suppressor of cytokine signalling; Kamura *et al.*, 1998). The SOCS box is composed of about 40 amino acids and is responsible for intermolecular recognition by forming three α -helices that form the binding interface for elongin BC (Stebbins *et al.*, 1999; Bullock *et al.*, 2007). The N-terminal portion of the SOCS box, which forms the first α -helix, was designated the 'BC box' because it was shown to be critical for interaction with elongin BC (Aso *et al.*, 1996; Kamura *et al.*, 1998). While elongin BC is the common adaptor for Cul2 and Cul5, it has been suggested that whether elongin BC binds to Cul2 or Cul5 is determined by the substrate receptors (Kamura *et al.*, 2004). For example, elongin BC in complex with von Hippel–Lindau tumour suppressor protein (VHL) interacts with Cul2 but not with Cul5, whereas elongin BC in complex with another SOCS-box protein, SOCS2, showed the opposite binding specificity (Kile *et al.*, 2002; Kamura *et al.*, 2004). Consistently, VHL-mediated degradation of HIF-2 α could be inhibited by RNAi-mediated knockdown of the Cul2–Rbx1 complex but not by knockdown of the Cul5–Rbx2 complex (Kamura *et al.*, 2004). Based on an experiment in which a peptide segment was swapped between VHL and SOCS2, an \sim 16-amino-acid segment C-terminal to the common BC box was defined as the determinant of the recognition specificity and this segment was consequently named the Cul2 or Cul5 box. The Cul5 box has the consensus sequence φ xxLP φ Pxx φ xx(Y/F)(L/I) (where φ is a hydrophobic residue and x is any residue; Hilton *et al.*, 1998; Kamura *et al.*, 2004), in which the conserved LP φ P motif was proposed to be the major determinant of specificity (Kamura *et al.*, 2004). Recently, an extensive cell-based protein-binding study identified 17 Cul2-interacting and 19 Cul5-interacting human

substrate receptors, allowing comparison of a large collection of these proteins (Mahrouf *et al.*, 2008). According to this study, a unique sequence motif distinguishing the two cullin boxes is not present, suggesting that all of the cullin box residues collectively contribute to the selective or preferential recognition of Cul2 or Cul5.

Whereas the ECS complexes composed of elongin BC, Cul2/Cul5 and a SOCS-box protein constitute a representative subfamily of cullin-dependent ubiquitin ligases (Kamura *et al.*, 2004), structural information of the intersubunit interaction is limited to elongin BC and a substrate receptor. In particular, it is unknown how a substrate receptor bound to elongin BC may direct this ternary complex to selectively or preferentially recognize Cul2 or Cul5. Here, we provide an atomic view of the intersubunit interactions between elongin BC, SOCS2 and an N-terminal fragment of Cul5. The structure readily explains why the elongin BC adaptor selectively pairs with Cul2 and Cul5 but not with other cullins. We have identified a ring-to-ring interaction which is important for tight interaction between Cul5 and the Cul5 box.

2. Experimental procedures

2.1. Cloning and protein purification

The DNA fragments encoding mouse elongin B and elongin C (residues 17–112) were ligated into the pRSFDuet plasmid (Novagen). The DNA fragment encoding human SOCS2 (residues 32–198) was ligated into the pProEx HTa plasmid (Invitrogen) and that encoding human Cul5 (residues 1–386) was ligated into a pET22b-CPD 10H plasmid which was designed to express a protein fused to a His₁₀-tagged CPD (cysteine protease domain) at the C-terminus. In this work, elongin C (residues 17–112), SOCS2 (residues 32–198) and Cul5 (residues 1–386) are referred to as elongin C, SOCS2 and Cul5N, respectively. A variant of Cul5N, referred to as Cul5N(RD), which contains the substitutions V341R and L345D, was generated by the overlapping PCR method. SOCS2, elongin B and elongin C were coexpressed together in *Escherichia coli* strain BL21 (DE3) (Stratagene) and Cul5N(RD) was expressed alone in *E. coli* strain BL21 (DE3) RIPL (Stratagene). Expression of the proteins was induced by 0.5 mM isopropyl β -D-1-thiogalactopyranoside at 291 K. Cell lysates were prepared by sonication in buffer A composed of 20 mM Tris–HCl pH 7.5, 100 mM NaCl. The SOCS2–elongin BC complex was purified using HisPur Cobalt Resin (Thermo Scientific) and a HiTrap Q anion-exchange column (GE Healthcare) operated with a linear NaCl gradient (0.0–1.0 M) in buffer A. Cul5N(RD) was first purified using HisPur Cobalt Resin, on which the CPD–His₁₀ tag was cleaved by adding 100 μ M phytate. Subsequently, the protein was bound to a HiTrap Q column and eluted with a linear gradient of NaCl (0.0–1.0 M) in buffer A. Purified SOCS2–elongin BC and Cul5N(RD) were mixed together in a 1:1 molar ratio and the resulting quaternary complex was further purified in buffer A using a HiLoad Superdex 200 gel-filtration column (GE Healthcare). The final sample was concentrated to 40 mg ml⁻¹

Table 1

Data-collection and structure-refinement statistics.

Values in parentheses are for the highest resolution shell.

Data collection	
Space group	C222 ₁
Unit-cell parameters (Å, °)	$a = 138.85$, $b = 141.46$, $c = 182.00$, $\alpha = \beta = \gamma = 90$
Wavelength (Å)	1.0000
Resolution (Å)	50.0–3.0
R_{merge} (%)	7.6 (35.7)
$\langle I/\sigma(I) \rangle$	23.0 (3.4)
Completeness (%)	97.3 (93.7)
Multiplicity	9.0 (4.6)
Refinement	
Resolution (Å)	50.0–3.0
No. of reflections	35501
$R_{\text{work}}/R_{\text{free}}$ (%)	22.5/24.8
R.m.s. deviations	
Bond lengths (Å)	0.0006
Bond angles (°)	1.3
Average B value (Å ²)	73.7
Ramachandran plot, residues in (%)	
Favoured regions	88.0
Additionally allowed regions	11.7
Generously allowed regions	0.3

in a buffer solution consisting of 25 mM Tris–HCl pH 7.5, 100 mM NaCl, 5 mM dithiothreitol.

A variant of Cul5N(RD) containing a W53A mutation, Cul5N(RD;W53A), was generated by the overlapping PCR method and the mutation was confirmed by DNA sequencing. The variant was purified according to the same procedures as used to purify Cul5N(RD). A DNA fragment encoding human VHL (residues 54–213; referred to as VHL) was amplified by PCR and cloned into the pProEx HTa vector. VHL, elongin B and elongin C were coexpressed together in *E. coli* strain BL21 (DE3) at 310 K and the purification steps for VHL–elongin BC were identical to those for SOCS2–elongin BC.

2.2. Crystallization and structure determination of SOCS2–elongin BC–Cul5N(RD)

Crystals of the quaternary complex were obtained by the hanging-drop vapour-diffusion method at 295 K by mixing and equilibrating 1.5 µl protein sample and 1.5 µl precipitant solution consisting of 0.25 M sodium citrate, 18% (w/v) PEG 3350. For cryoprotection, the crystals were soaked in the precipitant solution containing an additional 10% ethylene glycol. An X-ray diffraction data set was collected on beamline 17A at the Photon Factory in Japan. The asymmetric unit of the crystal contained one quaternary complex. The structure of the complex was determined by molecular replacement using the structures of SOCS2–elongin BC (PDB entry 2c9w; Bullock *et al.*, 2006) and Cul5N(RD) (PDB entry 2wzk; J. R. C. Muniz, V. Ayinampudi, Y. Zhang, J. J. Babon, A. Chaikuad, T. Krojer, A. C. W. Pike, M. Vollmar, F. Von Delft, C. H. Arrowsmith, A. M. Edwards, J. C. Weigelt, C. Bountra & A. Bullock, unpublished work) as the search models using *MOLREP* in the *CCP4* suite (Vagin & Teplyakov, 2010; Winn *et al.*, 2011). Structure refinement was carried out using the *CNS* software package (Brünger *et al.*, 1998). The final refined model does not include residues 105–118 of elongin B, resi-

dues 1–9 and 119–128 of Cul5N(RD) and residues 136–145 of SOCS2, for which electron density was missing. Crystallographic data statistics are summarized in Table 1.

2.3. Isothermal titration calorimetry

All measurements were carried out at 298 K on an iTC200 microcalorimetry system (GE Healthcare). Protein samples were dialyzed against a solution consisting of 20 mM Tris–HCl pH 7.5, 10 mM NaCl and were centrifuged to remove any insoluble material prior to the measurements. The experiments were carried out by titrating 1 mM Cul5N(RD) or Cul5N(RD;W53A) into 0.1 mM SOCS2–elongin BC or VHL–elongin BC. Dilution enthalpies were determined in separate experiments (titrant into buffer) and were subtracted from the enthalpies of binding between the proteins. The data were analyzed using the *Origin* software (OriginLab).

2.4. Simulation of the interaction between VHL, elongin BC and Cul2

Three-dimensional structural models of the complex between VHL–elongin BC and the N-terminal part of Cul2, referred to as Cul2N, were generated based on a high-accuracy template-based modelling method (Joo *et al.*, 2007). The template structures used for modelling VHL, elongin BC and Cul2N were VHL–elongin BC (PDB entry 1vcb; Stebbins *et al.*, 1999), SOCS2–elongin BC–Cul5N(RD) and Cul5N(RD) (PDB entry 2wzk). The method is based on global optimization of various scoring functions (Lee *et al.*, 2003) coupled with successive screening of models by quality assessment. It carries out multiple stages of optimization, including multiple sequence alignment, three-dimensional chain building of proteins and side-chain refinement. The final three-dimensional model of each target sequence was selected by applying a quality-assessment procedure which is based on a machine-learning algorithm using scoring functions and structural features such as the secondary structure and solvent accessibility of protein structures. The VHL–elongin BC and Cul2N models were initially oriented according to the structure of SOCS2–elongin BC–Cul5N(RD). The intersubunit interactions were optimized using the *TINKER* package (Ponder & Richards, 1987), which carries out molecular modelling based on potential energy functions using the CHARMM force field (MacKerell *et al.*, 1998) and the GBSA solvation model (Qiu *et al.*, 1997).

3. Results and discussion

3.1. Overall structure of the quaternary SOCS2–elongin BC–Cul5N(RD) complex

To obtain structural information on the intersubunit interactions between a SOCS-box protein, elongin BC and Cul5, various protein constructs were prepared and the resulting complexes were subjected to crystallization. Finally, we obtained crystals of the quaternary complex between elongin BC, SOCS2 and Cul5N(RD). We employed an N-terminal 386-amino-acid fragment of Cul5 (Fig. 1a) because the

N-terminal part of cullins is the region that interacts with the adaptor subunit, as demonstrated by various related structures (Zimmerman *et al.*, 2010). The two mutations in Cul5N(RD) are located on the otherwise completely hydrophobic surface, which is solvent-exposed owing to the truncation of the C-terminal half of Cul5. These mutations, which were introduced based on the available structure of this protein (PDB entry 2wzk), improved the solution behaviour of the protein. The four proteins were found to form a tight complex and the

crystal structure of this quaternary complex was determined to 3.0 Å resolution (Table 1). The Cul5N(RD) structure is composed exclusively of α -helices and looks like a curved rod. The adaptor subunit elongin BC sits at the N-terminal tip of Cul5N(RD) and the substrate receptor subunit SOCS2 binds to one side of elongin C (Fig. 1*b*). Elongin B, which forms a complex with elongin C, does not interact with Cul5N(RD) at all, whereas it interacts with SOCS2 only slightly *via* two residues (Val102 and Met103; not shown). We note that human elongin BC should interact with human SOCS2 and Cul5 in an identical manner to mouse elongin BC because both elongin B and elongin C share extremely high sequence homology (>97% identity) between the two species and the residues at the binding interfaces are invariant.

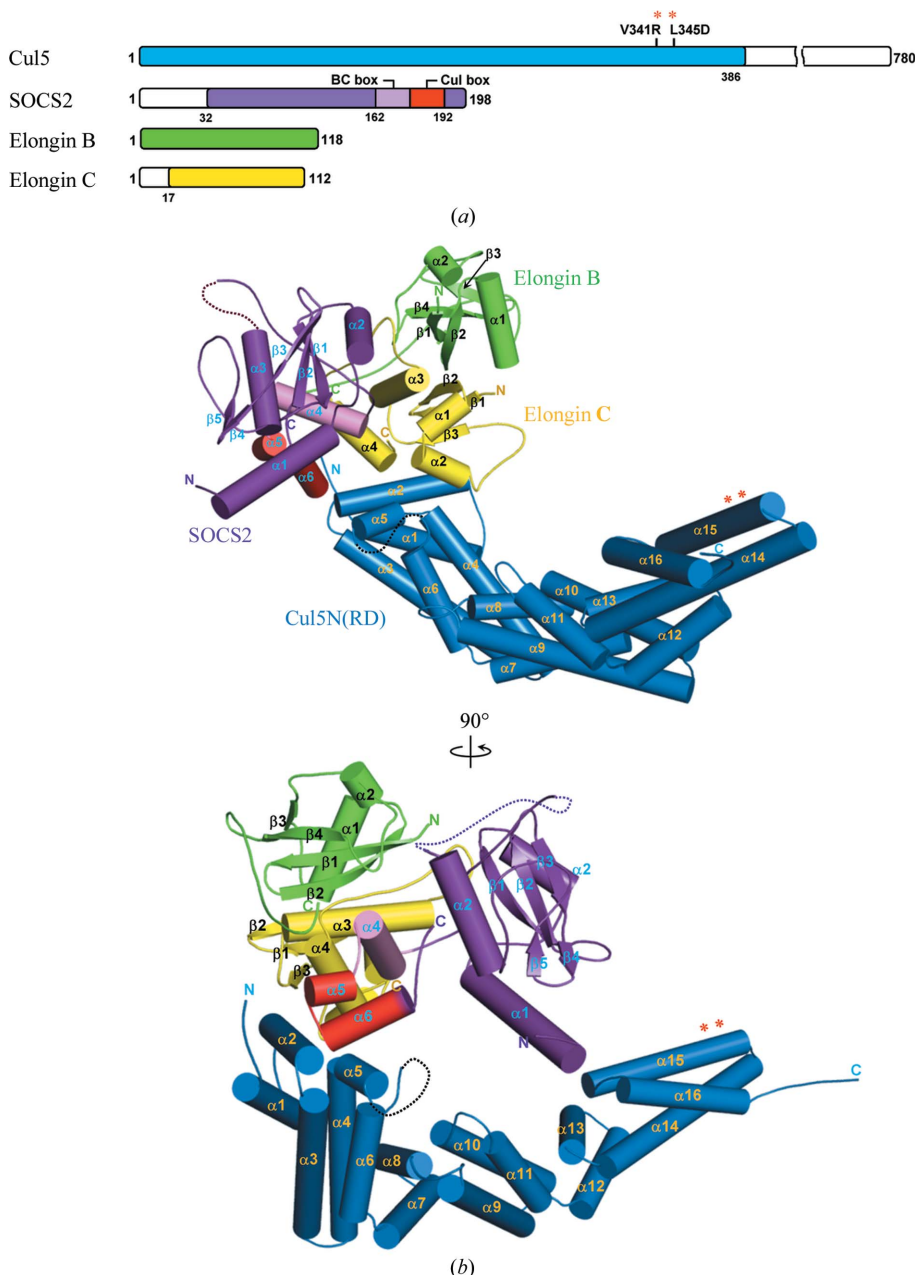


Figure 1
Overall structure of SOCS2–elongin BC–Cul5N(RD). (a) The primary-sequence diagrams indicate the constructs of the four proteins used for structure determination. The two hydrophilic substitutions in Cul5 are indicated. (b) The structure of the quaternary complex is shown in two orientations. The BC box and the Cul5 box in SOCS2 are indicated by pink and red colours, respectively. The positions of the hydrophilic substitutions are indicated by asterisks and the disordered regions are indicated by dotted lines.

3.2. Interface between elongin BC and Cul5

The binding of elongin BC to Cul5 takes place exclusively through elongin C. While $\alpha 4$ and $\alpha 5$ of Cul5 make minor contacts with elongin C *via* Ile106 and Lys109 on $\alpha 4$ and Gln113 on $\alpha 5$, $\alpha 2$ of Cul5 is the primary binding motif; it interacts with a shallow groove of elongin C formed by $\alpha 2$, loop $\alpha 2$ – $\beta 3$ and $\alpha 4$ (Fig. 2*a*). This intersubunit interaction is predominantly hydrophobic, but involves several hydrophilic interactions mediated by Ser47, Asn61 and Arg63 of elongin C, and Lys109, Gln38, Asp42 and Asp46 of Cul5. The mode of interaction between elongin BC and Cul5 is similar to that between Skp1 and Cul1 in the structure of the SCF complex composed of Skp1, Cul1–Rbx1 and the F-box protein Skp2 (PDB entry 1ldk; Zheng *et al.*, 2002). In this structure, Skp1 forms a binding interface using $\alpha 2$, the following 20-residue segment and $\alpha 5$, which interacts with $\alpha 2$ of Cul1 (Fig. 2*b*). However, the detailed intermolecular interactions in the two complexes are quite different, which can be ascribed to the amino-acid differences at the binding interfaces. A total of 12 residues of elongin C interact directly with $\alpha 2$ of Cul5 and ten residues of Skp1 interact directly with $\alpha 2$ of Cul1. Among the 12 residues of elongin C, only Met45 and Asn108 are identically conserved in Skp1 (Fig. 2*c*). Likewise, among the 11 residues of Cul5 which interact with elongin C, Lys37

is the sole residue that is identically conserved in the 12 residues of Cul1 (Fig. 2*d*). Owing to these differences, the two binding interfaces are quite different from each other electrostatically and geometrically. While the binding interface of Skp1 is almost flat, that of elongin C has two protrusions that are formed by Arg63 and by the Gly48-Pro49-Gly50 segment (Fig. 2*a*). The guanidine group of Arg63 is involved in ionic

interactions with Asp42 and Asp46 of Cul5, while Pro49 of elongin C is involved in hydrophobic interactions with Trp40 of Cul5 (Fig. 2*a*). Both Arg63 and Pro49 are not conserved in Skp1 and corresponding hydrophilic or hydrophobic interactions do not exist at the interface between Skp1 and Cul1. These geometric and electrostatic differences explain the selective binding of the two adaptors to Cul1 or Cul5.

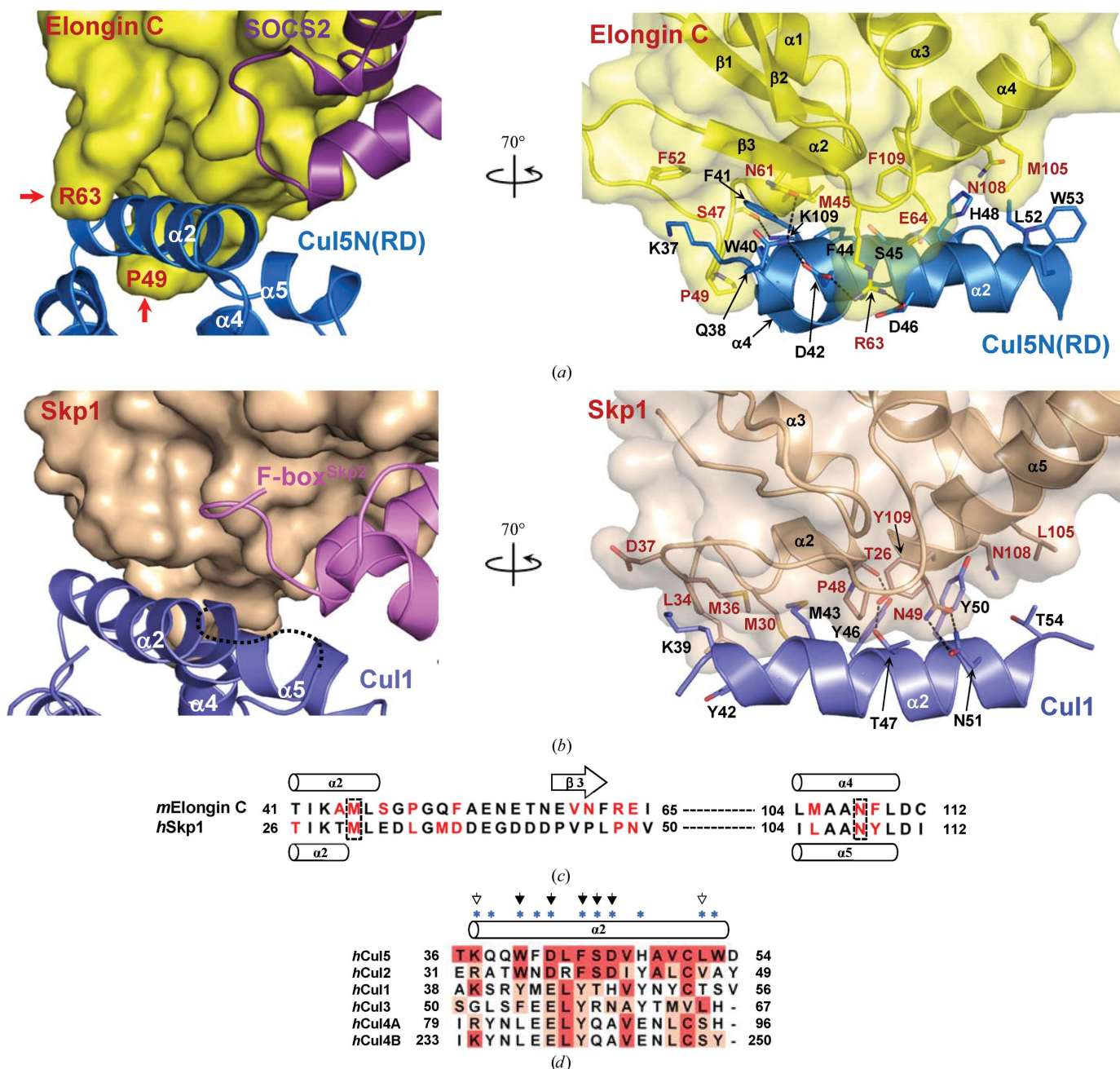
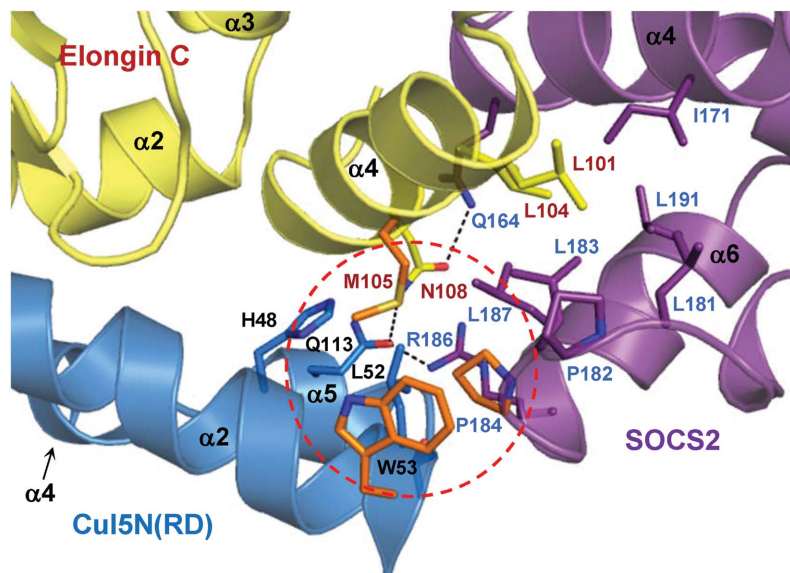


Figure 2

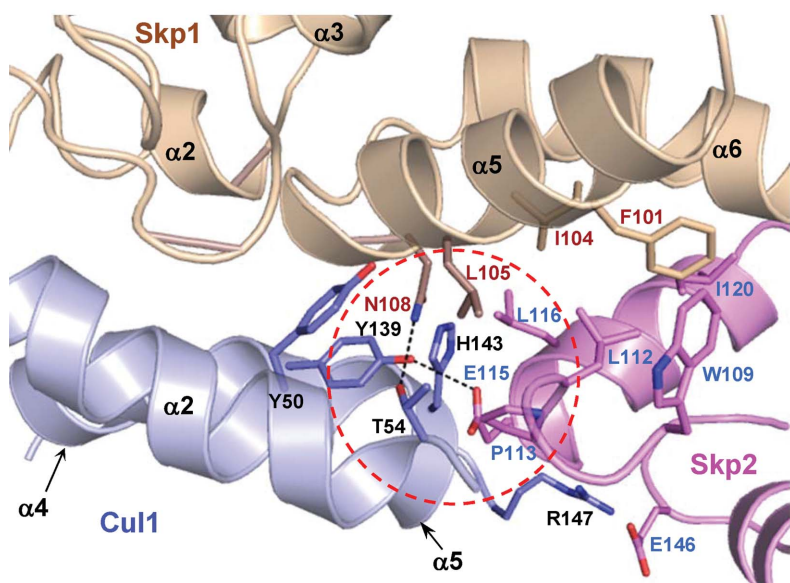
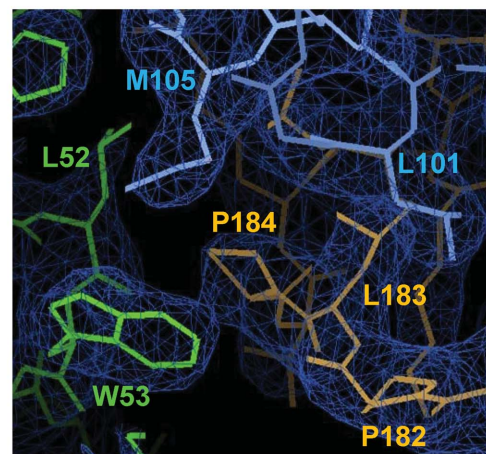
The binding interface between elongin C and Cul5. (a) The interface is shown in two orientations. The red arrows highlight that Arg63 and Pro49 of elongin C interact with $\alpha 2$ of Cul5 as if they grasp the helix. The stick presentation in the right panel indicates the residues involved in the intersubunit interaction (interatomic distance ≤ 4.0 Å). (b) For comparison, the interface between Skp1 and Cul1 (PDB entry 1ldk) is shown in two orientations. (c) The residues at the interface are not conserved. The sequences of elongin C and Skp1 are aligned and the two regions involved in the interaction with Cul5 or Cul1 are shown. The red letters indicate the Cul5N(RD)-contacting residues of elongin C and the Cul1-interacting residues of Skp1. Of these, only two residues, marked by dotted boxes, are conserved in the two proteins. (d) Sequence alignment of six different human cullins. The regions corresponding to $\alpha 2$ of Cul5 are shown. The asterisks indicate the Cul5 residues that interact directly with elongin C. These interacting residues are significantly more conserved in Cul2 (seven out of 11) than in any other cullins. Identically conserved residues in Cul5 and Cul2 are indicated by filled arrowheads and similarly conserved residues are represented by empty arrowheads.

Elongin BC serves as the adaptor for both Cul2 and Cul5 (Kamura *et al.*, 2004). The basis of this dual specificity can be explained by sequence comparison of the cullin-family proteins, which shows that the residues on the $\alpha 2$ helix of Cul5 which interact with elongin C are highly conserved in Cul2 but

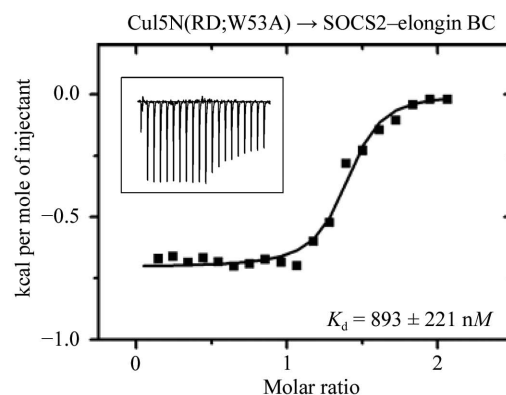
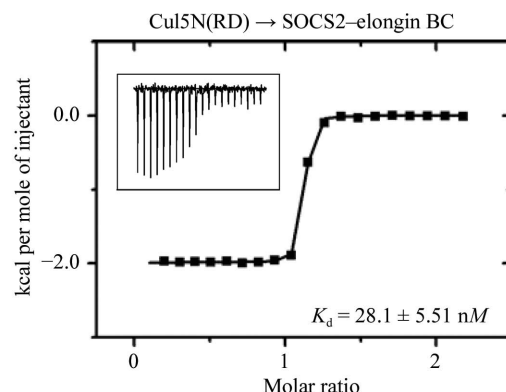
not in the other cullins. Among the 11 elongin C-interacting residues of Cul5, five residues (Trp40, Asp42, Phe44, Ser45 and Asp46) are identical in Cul2 and two further residues (Lys37 and Leu52) are similar (Fig. 2*d*). In contrast, only one residue (Lys37 or Leu52) is identical in Cul1, Cul3 and Cul4B



(a)



(b)



(c)

Figure 3

The binding interface between SOCS2 and Cul5. (a) The SOCS2–Cul5 interface is a part of a three-way interface between elongin C, SOCS2 and Cul5, which is indicated by the dotted circle. Each of the three residues in orange interacts with the other two residues simultaneously. The ring-to-ring interaction between Pro184 of SOCS2 and Trp53 of Cul5 is shown together with the final $2F_o - F_c$ electron-density map at the 1σ level. (b) For comparison, the overall interactions between the F box of Skp2, Skp1 and Cul1 (PDB entry 1ldk) are shown. The spatial position of the Skp2–Cul1 interface (circled) is similar to that of the SOCS2–Cul5 interface. (c) ITC analysis. Cul5N(RD) or Cul5N(RD;W53A) was titrated into the indicated protein complexes. The K_d values were deduced from curve fittings of the integrated heat per mole of added protein (insets).

(Fig. 2*d*). We also note that the sequence conservation in the $\alpha 2$ helices of Cul2 and Cul5 (41% identity and 65% similarity) is considerably higher than the overall sequence conservation between the two proteins (26% identity and 47% similarity). Therefore, local sequence conservation at the binding interface appears to be the key basis underlying the dual specificity of the elongin BC adaptor for Cul2 and Cul5.

Elongin C is structurally similar to the Cul3-interacting BTB (bric-à-brac, tramtrack, broad-complex) domain (Petroski & Deshaies, 2005). Recently, it was shown that the N-terminal tip of Cul3 interacts with the BTB domain of SPOP (speckle-type POZ protein) and that helix $\alpha 2$ of Cul3 is the major interface for this intermolecular interaction (Errington *et al.*, 2012). The sequence alignment shown in Fig. 2(*d*) explains the recognition specificity between the structurally similar adaptor proteins and the cullin scaffolds.

3.3. Interface between SOCS2 and Cul5

The presented structure reveals that SOCS2 interacts with Cul5 through only two residues, Pro184 and Arg186, which belong to the Cul5 box (residues 178–192). Pro184 is in hydrophobic contact with Trp53 and Leu52, whereas Arg186 of SOCS2 is hydrogen-bonded to Gln113 of Cul5 (Fig. 3*a*). Arg186 is a variable residue in the Cul5 boxes and therefore the observed hydrogen bond does not represent a conserved interaction. In contrast, Pro184 is invariable and is the fourth residue in the LP ϕ P sequence motif of the Cul5 box, which has been shown by mutational analyses to be the major determinant specifying the assembly of the SOCS box-containing proteins into Cul5 (Kamura *et al.*, 2004). The fourth proline residue in this motif appears to be particularly important as a determinant of specificity. Whereas wild-type SOCS1 containing the sequence IPLN in the cullin box failed to interact with Cul5–Rbx2, a mutant SOCS1 with an IPLP sequence interacted with Cul5–Rbx2 (Kamura *et al.*, 2004). In the structure of the quaternary complex, Pro184 of SOCS2 is involved in a ring-to-ring stacking interaction with Trp53 of Cul5 (Fig. 3*a*). Notably, both apolar residues interact with Met105 of elongin C and thus the three residues together form a three-way interaction point (Fig. 3*a*). At this position, the ring-to-ring stacking interactions appear to augment the hydrophobic interactions between elongin C and Cul5 as they are part of the large hydrophobic core involving Pro182, Leu183 and Leu187 of SOCS2, Leu101, Leu104 and Met105 of elongin C and Leu52 of Cul5 (Fig. 3*a*). The observed interaction between the Cul5 box of SOCS2 and Cul5 is similar to that between the F-box of Skp2 and Cul1 in the structure of the Skp1–Cul1–Skp2 F-box complex (PDB entry 1ldk; Zheng *et al.*, 2002). The F-box also interacts with Cul1, but only slightly: three residues of Skp2 (Pro113, Glu115, Glu146) are in contact with Thr54, Tyr139, His143 and Arg147 of Cul1 (Fig. 3*b*). Furthermore, the binding interface is spatially similar to that between SOCS2 and Cul5 (Figs. 3*a* and 3*b*). Thus, the ECS and SCF ubiquitin ligases share a common mode of interaction between their substrate receptor and the cullin scaffold.

3.4. Contribution of the cullin box to the assembly of ECS complexes

Pro184 in the Cul5 box of SOCS2 is substituted by a valine in the Cul2 box of VHL, which also binds to elongin BC but is known to interact with Cul2 instead of Cul5 (Kamura *et al.*, 1999, 2004). On the other hand, Trp53 of Cul5 is substituted by an alanine in Cul2. These observations indicated that the ring-to-ring interaction between Pro184 and Trp53 is important, if not critical, for the recognition of Cul5 by Cul5 box-containing proteins. To evaluate the importance of this interaction, we generated a Cul5N(RD) variant containing a W53A mutation, designated Cul5N(RD;W53A). Using isothermal titration calorimetry (ITC), we then quantified the interactions of SOCS2–elongin BC with Cul5N(RD) or Cul5N(RD;W53A). SOCS2–elongin BC interacted potently with Cul5N(RD), with an apparent dissociation constant (K_d) of 28 nM (Fig. 3*c*). In comparison, SOCS2–elongin BC interacted with the Cul5N(RD;W53A) variant with a K_d of 893 nM (Fig. 3*c*). Therefore, the ring-to-ring interaction significantly enhances the binding affinity between SOCS2–elongin BC and Cul5.

3.5. Contribution of elongin BC to the assembly of ECS complexes

Since elongin C interacts with Cul5N(RD) much more extensively than does SOCS2 (Fig. 3*a*), elongin BC is likely to bind Cul5 with high affinity and to contribute majorly to the binding affinity between SOCS2–elongin BC and Cul5. However, free elongin BC did not seem to interact tightly with Cul5N(RD) on a native gel-based protein-binding assay (not shown). Consistently, an ITC analysis confirmed that they interact with each other with a K_d of 1.3 μ M (not shown), as similarly estimated by others (Babon *et al.*, 2009; Wolfe *et al.*, 2010). On the other hand, it was shown that while SOCS3 bound to elongin BC interacts with Cul5N tightly (K_d of 90 nM), the interaction between isolated SOCS3 and Cul5N was undetectably weak ($>10 \mu$ M; Babon *et al.*, 2008, 2009). This observation is consistent with the minor interaction between Cul5 and the Cul5 box found in the presented structure and indicates that this intersubunit interaction by itself is negligible in the formation of an ECS complex. Therefore, elongin BC and the Cul5 box contribute to the formation of an ECS complex synergistically rather than additively. A structural comparison of Cul5N(RD) in the complex with free Cul5N(RD) showed that the protein undergoes a negligible conformational change: the r.m.s.d. of the C^α atoms between the two states is only 0.64 Å. We also note that the binding of SOCS2–elongin BC to Cul5N(RD) is accompanied by almost no conformational change in elongin C; only minor changes in the side-chain conformations of three residues (Leu101, Met105 and Asn108) are observed in a structural comparison between SOCS2–elongin BC–Cul5N(RD) and SOCS2–elongin BC (Fig. 4). While the structure of free elongin BC is unavailable, we presume that elongin C is conformationally flexible in free elongin BC. In this scenario, free elongin BC has to lose conformational freedom to bind Cul5 and the accompanying entropic loss

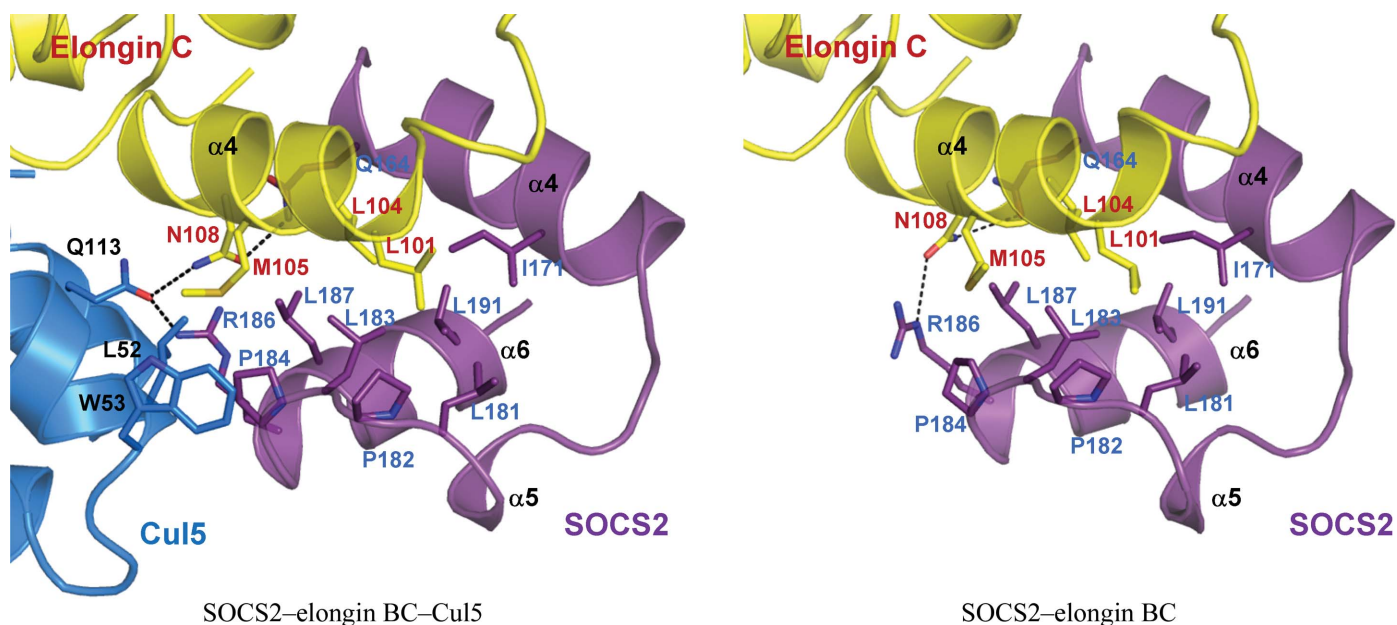


Figure 4 Negligible conformational change of elongin BC upon binding to Cul5N(RD). The elongin C molecules in the quaternary complex (left) and the triple complex (right; PDB entry 2c9w) are superposable with an r.m.s.d. of 0.88 Å (for all atoms). At the binding interfaces, conformational change of elongin C is restricted to the three side chains of Leu101, Met105 and Asn108. Dotted lines indicate hydrogen bonds.

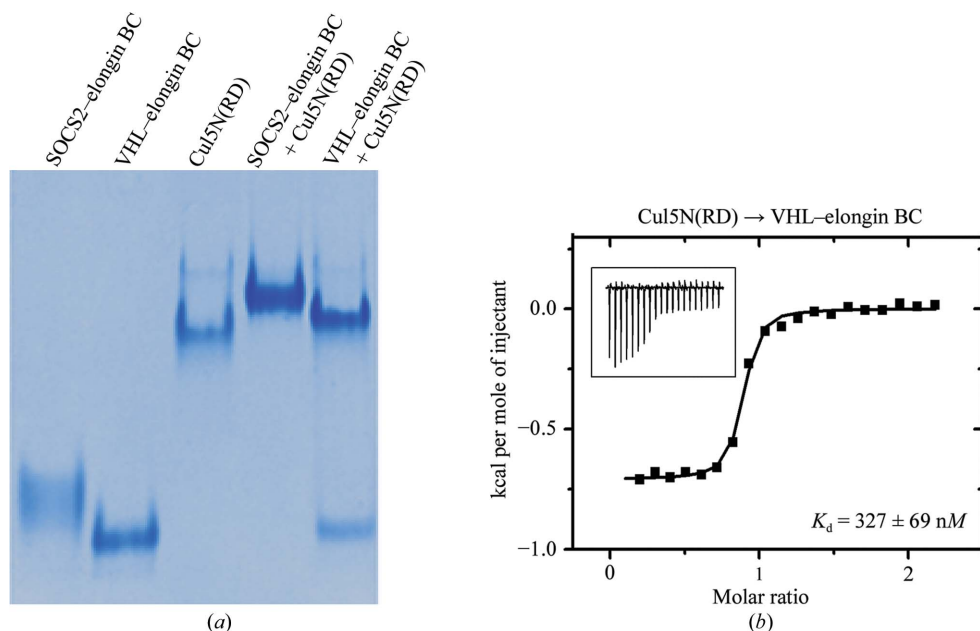


Figure 5 Interactions between VHL-elongin BC and Cul5. (a) PAGE. SOCS2-elongin BC or VHL-elongin BC, both at 6.7 μM, were incubated with 6.7 μM Cul5N(RD) at room temperature. The mixtures were loaded onto a native gel and visualized by Coomassie staining. Note the presence of a residual VHL-elongin BC band in lane 5 in comparison with the lack of a residual SOCS2-elongin BC band in lane 4. (b) ITC. VHL-elongin BC was titrated into Cul5N(RD) and the K_d value was deduced.

adversely affects the otherwise tight interaction between elongin BC and Cul5N(RD). In contrast, when elongin BC in complex with SOCS2 binds to Cul5, the loss of conformational freedom of elongin C is negligible. As a result, elongin BC in complex with a substrate receptor, but not free elongin BC, is able to bind Cul5 tightly, making a greater contribution to the overall binding affinity than the Cul5 box. If this proposition is

correct then VHL-elongin BC, which contains a Cul2 box instead of a Cul5 box, would bind not only Cul2 but also Cul5 with substantial binding affinity. Indeed, interaction between VHL-elongin BC and Cul5N(RD) was clearly observed, although it was less tight than the interaction between SOCS2-elongin BC and Cul5N(RD) on a native gel (Fig. 5a, lanes 4 and 5) and from the K_d value (327 versus 28 nM; Fig. 5b).

3.6. Simulation of the interaction between the Cul2 box of VHL, elongin C and Cul2

According to the published data, VHL-elongin BC would be presumed to bind Cul2 more tightly than it binds Cul5. Interestingly, a multiple sequence alignment shows that the BC box sequences in the SOCS boxes are

quite different from those in the VHL boxes, apart from the conservation of a leucine residue which corresponds to Leu163 in SOCS2 (Fig. 6a). We considered whether this sequence difference might cause a conformational difference in elongin C depending on its binding to VHL or to SOCS2. A structural comparison between VHL-elongin BC and SOCS2-elongin BC exhibited no noticeable conformational difference

in elongin C (r.m.s.d. of 0.29 on C^α atoms), indicating that the sequence difference in the BC box does not play a role in the preferential binding of VHL–elongin BC to Cul2. The residues that are conserved in the Cul2 box also do not appear to be a determinant, as they are also conserved in the Cul5 box (Fig. 6*a*). To understand the basis of this preferential binding, we attempted to crystallize a complex between VHL–elongin BC and an N-terminal fragment of Cul2. However, a number of the N-terminal fragments of Cul2 that we designed were only produced in insoluble forms. We instead sought to obtain a

structural model of the VHL–elongin BC–Cul2N complex by a high-accuracy template-based modelling method (Joo *et al.*, 2007) mainly based on the structure presented here. Compared with the structure of VHL–elongin BC (Stebbins *et al.*, 1999), the simulated quaternary structure shows that the loop containing the Leu178–Asp179–Ile180–Val181 sequence of the Cul2 box, which corresponds to the LP ϕ P motif in the Cul5 box, undergoes a conformational shift towards Cul2 (Fig. 6*b*; left). As a result, Val181 and Ser183 of VHL interact with Ala48 and Val47 of Cul2, respectively. Owing to this move-

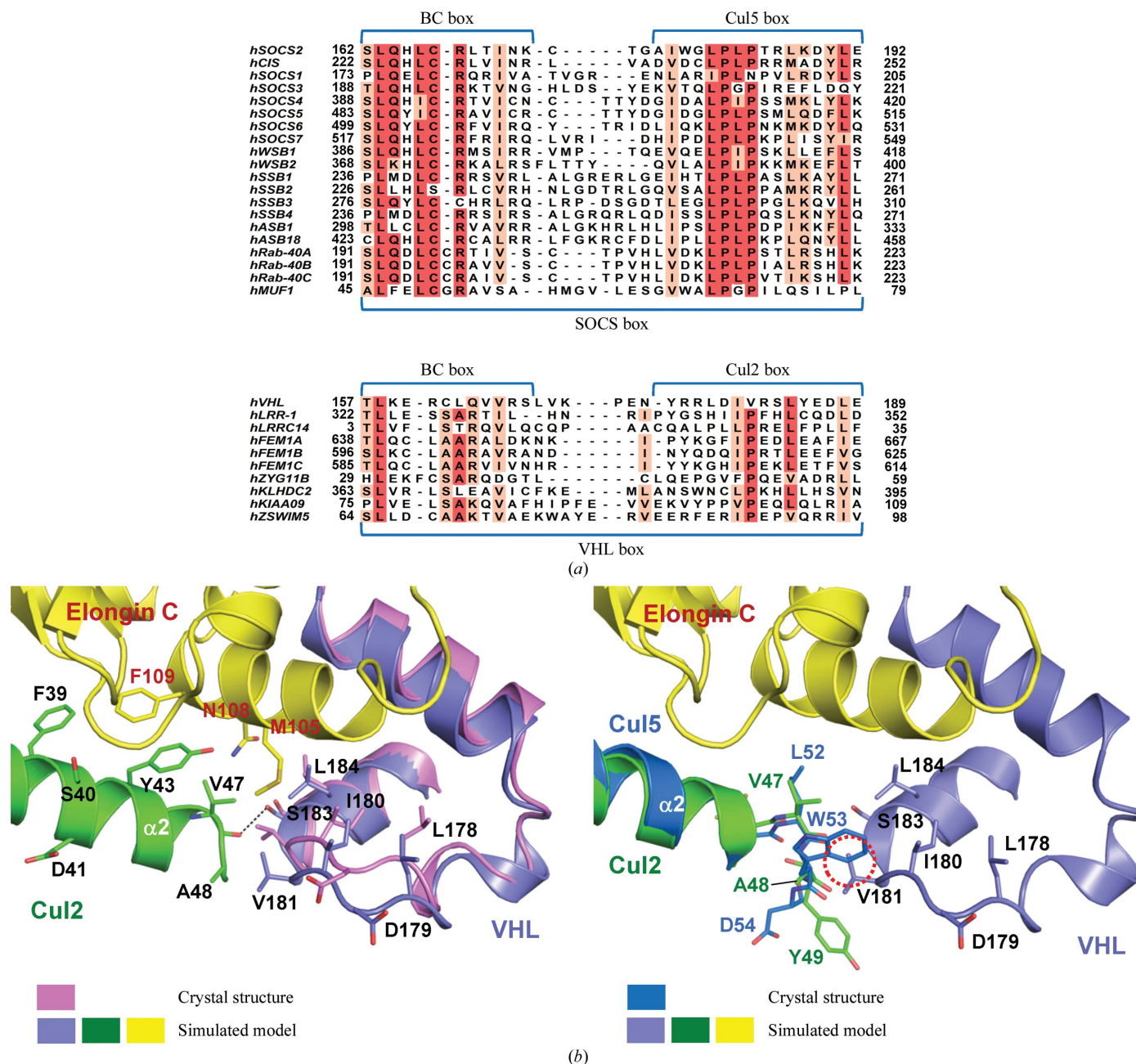


Figure 6 Simulated interaction between VHL–elongin BC and Cul2. (a) Sequence alignment of 30 of a total of 37 SOCS boxes and 20 VHL boxes that have recently been identified (Mahrouf *et al.*, 2008; Okumura *et al.*, 2012). It is noted that the Cul2-box-containing SOCS-box proteins are called VHL-box proteins (Kamura *et al.*, 2004; Hilton *et al.*, 1998). (b) Left: the loop segment of VHL becomes closer to $\alpha 2$ of Cul2 and forms a buried hydrogen bond. VHL in the structure of VHL–elongin BC (PDB entry 1vcv) is superposed on the simulated structures. Right: superposition of the $\alpha 2$ helix of Cul5N(RD) on the simulated structures. The circle highlights that Trp53 of Cul5 clashes sterically with Val181 of VHL, with a closest distance of 0.5 Å.

ment, the hydrophobic residues around Val181 of VHL become more closely packed against each other. In addition, a strong hydrogen bond appears to be formed between the hydroxyl group of Ser183 and the carbonyl O atom of Val47, which are completely buried in the hydrophobic milieu. These interactions between the Cul2 box of VHL and Cul2 should augment the interaction between elongin BC and Cul2. On the other hand, the Cul2 box would interact with Cul5 less preferably owing to the amino-acid dissimilarity between Cul2 and Cul5 near the three-way interface. In particular, Leu52 and Trp53 in Cul5, which are bulkier than the corresponding Val47 and Ala48 in Cul2, appear to prevent the conformational shift of the Cul2 box and thus the formation of the favourable Cul2–Cul2 box interactions observed in the simulated structure (Fig. 6*b*; right).

The simulated interactions between VHL and Cul2 do not provide a general explanation as to why the Cul2 box preferentially interacts with Cul2 rather than Cul5. This is because Val181 of VHL is mostly substituted by proline in other VHL-box proteins and Ser183 is not a conserved residue in other Cul2 boxes (Fig. 6*a*). Notably, the Cul2 box is far more diverse in primary sequence than the Cul5 box (Fig. 6*a*). It is possible that owing to the smaller residues in $\alpha 2$ of Cul2 (Val47 and Ala48 instead of leucine and tryptophan), this helix is able to make favourable interactions with the loop segment of different Cul2 boxes in different ways, such that unconserved interactions between each Cul2 box and Cul2 are responsible for the preferential binding to Cul2 over Cul5.

4. Summary and concluding remarks

The structure presented in this study provides the first atomic views of how elongin BC and a cullin box of a substrate receptor interact with a cullin. The elongin BC adaptor interacts selectively with Cul2 and Cul5 because the residues at the binding interface are conserved in these two cullins but not in other cullins. Elongin BC, which interacts with Cul5 much more extensively than the Cul5 box, is the major contributor to the overall binding affinity for the interaction between SOCS2–elongin BC and Cul5. The ring-to-ring interaction between Cul5 and the Cul5 box appears to be minor but contributes significantly to the overall binding affinity. Such a single critical interaction does not appear to exist in the interaction between Cul2 and the VHL-box proteins. Finally, our analyses indicate that a complex between substrate receptor and elongin BC is formed first and this complex then interacts with the Cul2–Rbx1 or Cul5–Rbx2 scaffold to assemble an ECS E3 ligase complex.

The authors declare no conflicts of interest. This work was supported by the GRL Program (K20815000001) from the National Research Foundation of Korea and made use of beamline 5C at the Pohang Accelerator Laboratory in Korea and beamline 17A at the Photon Factory in Japan. KJ and JL were supported by a National Research Foundation grant funded by the Korean government (No. 20120001222). We

thank the KIAS Center for Advanced Computation for providing computing resources.

References

- Aso, T., Haque, D., Barstead, R. J., Conaway, R. C. & Conaway, J. W. (1996). *EMBO J.* **15**, 5557–5566.
- Babon, J. J., Sabo, J. K., Soetopo, A., Yao, S., Bailey, M. F., Zhang, J.-G., Nicola, N. A. & Norton, R. S. (2008). *J. Mol. Biol.* **381**, 928–940.
- Babon, J. J., Sabo, J. K., Zhang, J.-G., Nicola, N. A. & Norton, R. S. (2009). *J. Mol. Biol.* **387**, 162–174.
- Bai, C., Sen, P., Hofmann, K., Ma, L., Goebel, M., Harper, J. W. & Elledge, S. J. (1996). *Cell*, **86**, 263–274.
- Bosu, D. R. & Kipreos, E. T. (2008). *Cell Div.* **3**, 7.
- Brünger, A. T., Adams, P. D., Clore, G. M., DeLano, W. L., Gros, P., Grosse-Kunstleve, R. W., Jiang, J.-S., Kuszewski, J., Nilges, M., Pannu, N. S., Read, R. J., Rice, L. M., Simonson, T. & Warren, G. L. (1998). *Acta Cryst.* **D54**, 905–921.
- Bullock, A. N., Debreczeni, J. É., Edwards, A. M., Sundstrom, M. & Knapp, S. (2006). *Proc. Natl Acad. Sci. USA*, **103**, 7637–7642.
- Bullock, A. N., Rodriguez, M. C., Debreczeni, J. É., Songyang, Z. & Knapp, S. (2007). *Structure*, **15**, 1493–1504.
- Dias, D. C., Dolios, G., Wang, R. & Pan, Z.-Q. (2002). *Proc. Natl Acad. Sci. USA*, **99**, 16601–16606.
- Duan, D. R., Pause, A., Burgess, W. H., Aso, T., Chen, D. Y., Garrett, K. P., Conaway, R. C., Conaway, J. W., Linehan, W. M. & Klausner, R. D. (1995). *Science*, **269**, 1402–1406.
- Errington, W. J., Khan, M. Q., Bueler, S. A., Rubinstein, J. L., Chakrabarty, A. & Privé, G. G. (2012). *Structure*, **20**, 1141–1153.
- Hershko, A. & Ciechanover, A. (1992). *Annu. Rev. Biochem.* **61**, 761–807.
- Hilton, D. J., Richardson, R. T., Alexander, W. S., Viney, E. M., Willson, T. A., Sprigg, N. S., Starr, R., Nicholson, S. E., Metcalf, D. & Nicola, N. A. (1998). *Proc. Natl Acad. Sci. USA*, **95**, 114–119.
- Joo, K., Lee, J., Lee, S., Seo, J.-H. & Lee, S. J. (2007). *Proteins*, **69**, Suppl. 8, 83–89.
- Kamura, T., Koepp, D. M., Conrad, M. N., Skowyra, D., Moreland, R. J., Iliopoulos, O., Lane, W. S., Kaelin, W. G., Elledge, S. J., Conaway, R. C., Harper, J. W. & Conaway, J. W. (1999). *Science*, **284**, 657–661.
- Kamura, T., Maenaka, K., Kotoshiba, S., Matsumoto, M., Kohda, D., Conaway, R. C., Conaway, J. W. & Nakayama, K. I. (2004). *Genes Dev.* **18**, 3055–3065.
- Kamura, T., Sato, S., Haque, D., Liu, L., Kaelin, W. G., Conaway, R. C. & Conaway, J. W. (1998). *Genes Dev.* **12**, 3872–3881.
- Kile, B. T., Schulman, B. A., Alexander, W. S., Nicola, N. A., Martin, H. M. & Hilton, D. J. (2002). *Trends Biochem. Sci.* **27**, 235–241.
- Lee, J., Lee, I.-H. & Lee, J. (2003). *Phys. Rev. Lett.* **91**, 080201.
- Liu, J. & Nussinov, R. (2011). *J. Biol. Chem.* **286**, 40934–40942.
- MacKerell, A. D. *et al.* (1998). *J. Phys. Chem. B*, **102**, 3586–3616.
- Mahrouf, N., Redwine, W. B., Florens, L., Swanson, S. K., Martin-Brown, S., Bradford, W. D., Staehling-Hampton, K., Washburn, M. P., Conaway, R. C. & Conaway, J. W. (2008). *J. Biol. Chem.* **283**, 8005–8013.
- Ohta, T., Michel, J. J., Schottelius, A. J. & Xiong, Y. (1999). *Mol. Cell*, **3**, 535–541.
- Okumura, F., Matsuzaki, M., Nakatsukasa, K. & Kamura, T. (2012). *Front. Oncol.* **2**, 10.
- Petroski, M. D. & Deshaies, R. J. (2005). *Nature Rev. Mol. Cell Biol.* **6**, 9–20.
- Pickart, C. M. (2001). *Annu. Rev. Biochem.* **70**, 503–533.
- Ponder, J. W. & Richards, F. M. (1987). *J. Comput. Chem.* **8**, 1016–1024.
- Ponyeam, W. & Hagen, T. (2012). *Cell. Signal.* **24**, 290–295.
- Qiu, D., Shenkin, P. S., Hollinger, F. P. & Still, W. C. (1997). *J. Phys. Chem. A*, **101**, 3005–3014.

- Stebbins, C. E., Kaelin, W. G. & Pavletich, N. P. (1999). *Science*, **284**, 455–461.
- Tan, P., Fuchs, S. Y., Chen, A., Wu, K., Gomez, C., Ronai, Z. & Pan, Z.-Q. (1999). *Mol. Cell*, **3**, 527–533.
- Vagin, A. & Teplyakov, A. (2010). *Acta Cryst.* **D66**, 22–25.
- Villeneuve, N. F., Lau, A. & Zhang, D. D. (2010). *Antioxid. Redox Signal.* **13**, 1699–1712.
- Winn, M. D. *et al.* (2011). *Acta Cryst.* **D67**, 235–242.
- Wolfe, L. S., Stanley, B. J., Liu, C., Eliason, W. K. & Xiong, Y. (2010). *J. Virol.* **84**, 7135–7139.
- Zheng, N., Schulman, B. A., Song, L., Miller, J. J., Jeffrey, P. D., Wang, P., Chu, C., Koepp, D. M., Elledge, S. J., Pagano, M., Conaway, R. C., Conaway, J. W., Harper, J. W. & Pavletich, N. P. (2002). *Nature (London)*, **416**, 703–709.
- Zimmerman, E. S., Schulman, B. A. & Zheng, N. (2010). *Curr. Opin. Struct. Biol.* **20**, 714–721.